PNL-SA--20796

DE92 041333

GEOHYDROLOGIC CHARACTERIZATION FOR AQUIFER THERMAL ENERGY STORAGE

S. H. Hall
J. R. Raymond

August 1992

Presented at the 1992 Intersociety
Energy Conversion Engineer Conference
August 3-7, 1992
San Diego, California

Prepared for
the U.S. Department of Energy
under Contract DE-AC06-76RLO 1830

Pacific Northwest Laboratory
Richland, Washington

ABSTRACT

Successful operation of an aquifer thermal energy storage system depends on three elements: 1) the presence of a suitable aquifer for ground-water supply and energy storage; 2) the availability of a source of free or low-cost thermal energy, such as industrial waste heat or environmental chill; and 3) a temporal mismatch between thermal energy availability and thermal energy use. Using conventional hydrogeologic methods for aquifer characterization, the presence of a suitable aquifer is the most difficult of these three elements to assess quantitatively. By combining conventional methods with drift-and-pumpback and point-dilution single-well tracer tests, however, the rate of ground-water flow, the effective porosity, and the vertical distribution of hydraulic conductivity of the aquifer can be estimated quickly and economically.

INTRODUCTION

Storing thermal energy in ground-water systems (aquifers) is an energy conservation concept designed to partly replace costly or scarce primary energy sources, such as petroleum, with abundant and inexpensive heat or chill. For example, industrial waste heat can be stored in an aquifer for later use in comfort heating. Similarly, the chill of cold winter air can be stored for air conditioning during summer months. An aquifer thermal energy storage (ATES) system in its simplest form is composed of a pair (doublet) of fairly conventional water supply wells drilled into an aquifer. Geologic materials are good thermal insulators, and potentially suitable aquifers are widely available throughout the United States.

During operation of an ATES system, ground water is withdrawn from one well, heated or chilled in a heat exchanger, and then returned for storage to the same aquifer via a second well (Figure 1). For recovery of the stored thermal energy, the second well is pumped, and the hot or cold water is again circulated through a heat exchanger and then returned to the aquifer through the first well. The recovered thermal energy can be used for space or process heating or cooling, thus reducing the need for primary energy. The cycle is repeated on a seasonal or other temporal basis. The ATES system is simple, inexpensive, and relatively efficient.

Successful design and operation of an ATES system depend on three elements: 1) the presence of a suitable aquifer for ground-water supply and energy storage; 2) the availability of a source of free or low-cost thermal energy; and 3) a temporal mismatch between thermal energy availability and thermal energy use.

Element 1 is usually the most difficult component of an ATES system to assess quantitatively. In this paper, we present a practical and economic method for characterizing geohydrologic systems for ATES applications. The method combines conventional hydrologic testing with single-well geochemical tracer tests and is illustrated by a case study of an existing ATES installation in Tuscaloosa, Alabama.

Aquifer characterization is important to the engineering design of an ATES installation; that is, the aquifer must be considered as one important component of the ATES heating or cooling plant. However, unlike the pumps, heat exchangers, and other mechanical components of the system, the aquifer cannot be altered to meet design specifications. Thus, to some degree, the ATES plant must be designed to accommodate the aquifer.

For example, the capacity of the aquifer to accept or yield water limits the flow rate that can be used in an ATES plant. Also, the effective porosity of the aquifer affects the volume of aquifer required to store a given volume of heated or chilled water. This in turn affects the size of an ATES well field. The direction and rate of ground-water flow similarly affects the size, shape, and operation of the well field.

The aquifer's hydraulic conductivity, which is a measure of the ability of the porous geologic media to transmit water, is of first-order importance in design and evaluation of ATES systems, and is dependent on the size and shape of the media pores. Hydraulic conductivity (K) multiplied by aquifer thickness (b) equals aquifer transmissivity, which is a measure of the rate at which water moves through a unit width of the aquifer under a unit hydraulic gradient. A high hydraulic conductivity (and transmissivity) is desired to produce the largest volume of water from a well with the least drawdown of ground-water level. However, paradoxically, low hydraulic conductivity is desirable for decreased regional ground-water velocity and prevention of excessive tilting of the thermocline from viscosity/buoyancy effects in high-temperature ATES systems. Isotropic aquifer media (having the same hydraulic conductivity in all directions) are desirable to obtain maximum water supply from a well with minimum drawdown. But, conversely, anisotropic conditions (with vertical hydraulic conductivity being much less than horizontal hydraulic conductivity) are desirable for high-temperature ATES systems to resist tilting of the thermocline.

Porosity of geologic media is expressed as the ratio of the pore volume to the total volume of the rock. With regard to the storage and movement of water in a porous medium, only the system of interconnected interstices (effective porosity) is important. The porosity of the aquifer matrix is an

important consideration in ATES systems because it determines the amount of heated or chilled water that can be stored per unit volume of the aquifer. Porosity also is important because it is one factor that controls ground-water velocity. Ground-water velocity in a porous medium is proportional to the hydraulic conductivity and gradient (slope of the water table or piezometric surface) and inversely proportional to the porosity.

Areal aquifer boundaries and aquifer thickness determine the volume available for storage of heat or chill. Aquifer volume generally is much greater than the required storage volume, but boundary location may be of interest if the proposed ATES storage site is near zones of recharge or discharge, or on the periphery of a ground-water system.

Thermal characteristics of the aquifer are important in determining the heat capacity of the system and conduction of heat out of the storage volume. Thermal conductivity is the quantity of heat conducted in unit time across an element of surface urder a given thermal gradient. Porous geologic materials, saturated with water, do not vary widely in thermal conductivity values. Basically, earth materials are good insulators under ATES conditions, and differences in their thermal conductivities are relatively small. Thus, thermal conductivity is of second-order importance in geohydrologic characterization. Thermal capacity (specific heat) of a material is the quantity of heat required to produce a unit change of temperature in a unit mass of media. Variation in thermal capacity of earth materials, as with thermal conductivity, is small, so characterizing thermal capacity is also of second-order importance.

The following case study is an example of a combined program of conventional and tracer testing. It also illustrates some methods and techniques for conducting the tracer tests. The testing methods presented here can be used to address all factors of aquifer characterization except for thermal characteristics of the aquifer.

EXPERIMENTAL

An ATES system has been in operation since 1985 at the University of Alabama Student Recreation Center (UASRC), located on the university campus in Tuscaloosa, Alabama. In this ATES system, ground water is circulated between heat exchangers and the unconfined aquifer via a well field consisting of six production wells. During cool months, the water is chilled and injected into the aquifer. During warm months, the stored water is withdrawn from the aquifer to serve as a heat sink to cool the air in the UASRC building. The production and water-level monitoring wells used for this test are shown in Figure 2.

In November 1991, Pacific Northwest Laboratory (PNL) conducted a series of field tests at the UASRC site to determine aquifer characteristics including the direction and rate of ground-water flow, formation effective porosity, hydraulic conductivity, vertical distribution of flow within the aquifer, and the specific capacity of wells during both injection and withdrawal (Hall and Newcomer, 1992). The purpose of this series of tests was to provide design data for expansion of the well field.

The unconfined aquifer at the UASRC site is within unconsolidated alluvium consisting of sands, gravels, and clays from the nearby Black Warrior River (Schaetzle and Brett, 1989). These deposits are believed to be 10 to 30 thousand years old, formed during the final phases of the Wisconsin Glaciation. The sediments overlie the Pottsville Formation, which consists of well-indurated shales and limestone, is of low permeability, and provides the lower boundary of the unconfined aquifer. In the vicinity of the test site, the sediments are typically 24 to 27 m thick, and the lower 9 to 12 m are saturated with ground water.

Production wells 1 through 6 were drilled with a 0.43-m (17-in.) diameter bit and completed through the sediments and slightly into the Pottsville Formation (Schaetzle and Brett, 1989). In each case, 0.25-m (10-in.) diameter PVC screen, with 8.1- x 10^{-4}-m (0.032-in.) openings, was installed in the lower 15.2 m of the well. The screen was gravel-packed to just above the screen/PVC casing connection, and then grouted with concrete to

the surface. Each well was developed by pumping for a period of approximately one day at a rate of 1.3×10^{-2} to 1.6×10^{-2} m^3/s. The monitoring wells were constructed using 0.051-m (2-in.) PVC casing, and screened and sand-packed near the bottom of the aquifer.

Hydraulic gradient and the direction of flow were determined from water-level measurements taken from well #1, well #4, and well #5, and from survey data provided by the University of Alabama. The water levels were measured from the top of the well casings with a steel tape just before the start of the aquifer tests. The resulting hydraulic gradient was 0.0045. The direction of flow relative to the layout of the well field is shown in Figure 2. A step-injection test was performed at well #1 to determine the injection capacity of a typical production well. Well #4 was used to supply water for injection at well #1, and pumping at well #4 was treated as a concurrent step-drawdown test. Pressure transducers were installed in both wells for monitoring water level change. The discharge end of the supply line leading from well #4 to well #1 was placed below water level in well #1 to prevent frothing and the resulting injection of entrapped air into the aquifer.

The test was started with an initial pumping rate of 5.0×10^{-3} m^3/s, increased in 2.5×10^{-3} m^3/s increments up to 1.26×10^{-2} m^3/s, and followed by a final increase to 1.77×10^{-2} m^3/s. Each increment was maintained for approximately one-half hour, except for the final pumping rate, which was maintained for approximately one hour. Figure 3 illustrates the changes in water level observed during the test. Note that after approximately 65 min of injection, during the 1.0×10^{-2} m^3/s flow step, the water level in well #1 rose above the level of the screen.

The specific capacity of each well was determined using the method of Jacob (1946), where change in water level is expressed as a function of flow as follows:

$$s = BQ + CQ^2 \qquad (1)$$

where s = drawdown in m

Q = flow rate in m^3/s

B = formation loss coefficient
C = well loss coefficient

The graphical method described by Driscoll (1986) was used to determine the values of the coefficients B and C. This method uses a rearranged form of EQ (1), where a best-fit straight line through a plot of s/Q vs Q yields a slope equal to C and an ordinate intercept equal to B. Figure 4 illustrates such plots for the test wells. At well #1, it is seen that, depending on flow rate, ground-water mounding will occur at the rate of approximately 500 to 600 m per m^3/s (~0.1 ft/gpm).

A constant discharge pumping test was started at well #4 approximately 18 h after completion of the step-injection test. Based on the results of the step-injection test, a discharge rate of 1.77×10^{-2} m^3/s was chosen, and that rate was maintained for a duration of 8 h. After pumping was stopped, water level recovery was monitored for 15 h.

Wells H2N and H3N, located 15.2 m and 19.5 m, respectively, from well #4, were used as the principal observation wells. Downhole pressure transducers were used to monitor drawdown and recovery in the pumping and observation wells. Near the end of the 8-h pumping phase of the test, the maximum drawdown observed in the pumping well was 6.94 m. Maximum drawdown in the observation wells was 1.14 m in well H2N, and 0.90 m in well H3N. The test data were corrected for aquifer dewatering prior to analysis using the following equation:

$$H = H' - (H'^2/2b) \qquad (2)$$

where H' = uncorrected drawdown in m
b = aquifer thickness, in m, prior to pumping

A combination of pressure derivatives (Bourdet et al. 1983; Bourdet et al. 1989), straight-line solutions (Jacob, 1946), and type-curve matching techniques (Theis, 1935; Novakowski, 1990) was applied to the corrected data to estimate values of transmissivity, storage coefficient, and specific yield.

Analysis of drawdown data yielded a value of storativity of 0.0002 to 0.0005, specific yield of approximately 0.1, and transmissivity of 280 m^2/day to 320 m^2/day. A similar analysis of recovery data confirmed these results.

Approximately 19 h after pumping ceased during the constant discharge test, a point-dilution test was initiated at well #4 by emplacing a bromide tracer into the well bore. A point-dilution test, as described by Kearl et al. (1988) is used to estimate ground-water velocity. (The rate at which the concentration of a tracer in a well bore decreases over time is a function of ground-water velocity.) For this test, point-dilution was used to estimate the distribution of flow velocities with depth by monitoring bromide concentrations at several depth intervals.

To emplace the tracer, a 1.6- x 10^{-2}-m (5/8-in.) ID hose, open at both ends, was suspended in the well to the bottom of the aquifer. The hose was weighted with a plastic jug having a radius of approximately 0.18 m. Gravel was added to the jug as ballast. The contained volume of the hose, from water table to the lower end, was 2.2 L; the volume of water used to dissolve 125 g of lithium bromide (LiBr). The solution was poured into the top of the hose, displacing well water from the hose. The hose was then withdrawn from the well, leaving the tracer solution in place. The jug used to weight the hose also served to mix the tracer within the well bore as the hose and jug were withdrawn.

Based on the 0.25-m well diameter and the 11.3-m effective aquifer thickness, the predicted bromide concentration immediately after tracer emplacement was 202 mg/L.

Following tracer emplacement, the bromide concentration in the well bore was monitored as a function of time and depth. Downhole measurements were made at 0.9-m (3-ft) intervals over a period of 5 h. The measurements were made using an Ag/AgBr ion-selective electrode and a submersible double-junction reference electrode of the Ag/AgCl type having an inner filling solution of 4 M KCl (saturated with AgCl) and an outer filling solution of 10% KNO_3. The reference electrode is of a new design, which was developed at PNL specifically for deep, in situ electrochemical measurements. The electrodes

were connected to a Hach One pH/millivolt meter with 30 m (100 ft) of dual-conductor insulated wire. Figure 5 illustrates the results of measurement.

The electrodes were calibrated just prior to the point-dilution test using a concentrated solution of lithium bromide and a sample of natural ground water collected from well #4. Well water spiked to a bromide concentration of 10 mg/L yielded a response of 62.1 mv. Based on previous testing, the bromide sensing electrode used in this experiment was known to consistently respond with -56 mv per decade of increasing concentration (i.e., 95% of the theoretical Nernst slope) in the range from 10 to 1000 mg/L. Therefore, millivolt readings for the test may be converted to bromide concentrations using the following equation:

$$A = 10^{(1+(62.1-E)/56)} \quad (3)$$

where A = bromide concentration in mg/L
E = millivolt reading

Inspection of Figure 5 shows that the bromide tracer was not quite evenly distributed at the time of emplacement. That is, the millivolt responses for each test depth, when extrapolated to zero time, are not all equal. The extrapolated potentials range from -8 to -16 mv. Each of these potentials represents a 0.9-m segment of well bore, except for the deepest test interval, which represents 1.2 m of well bore. Converting the zero-time potentials to bromide concentrations and weighting each according to the length of borehole segment that it represents yields a mean calculated bromide concentration of 206 mg/L. This compares quite favorably to the predicted concentration of 202 mg/L.

To calculate flow velocities, the following equation, modified from Hall et al. (1991a) with EQ (3) above, was used:

$$dE/dt = .0846V^* \quad (4)$$

where dE/dt = the slope of the plot of mv vs time in minutes
V* = ground-water flow velocity through the well bore in m/day

The theory describing a point-dilution test requires that, in a valid experiment, the slope dE/dt be a straight line (Hall et al., 1991a). Inspection of Figure 5 shows that, at all test depths, the data support a straight-line interpretation. (At some of the test depths, e.g., 8.7 m, there is some curvature in the plot of mv vs time early in the experiment. This curvature may have been caused by initial non-ideal distribution of the bromide tracer between the well bore and the gravel pack, which is effectively part of the well installation. Alternatively, the curvature may be an artifact of vertical mixing within the well bore caused by frequent movement of the sensing electrode assembly early in the experiment.) However, the theory also requires that the tracer be at all times evenly distributed in each test interval within the well bore. That is, mixing within the bore must be fast compared to the rate of ground-water flow through the bore. If this condition is not met, EQ (4) becomes invalid. A plot of mv vs time would then reflect a plug flow component, and the plot would tend toward a step function rather than a straight line.

In conventional practice, a point-dilution test is conducted by isolating a test interval, such as with packers, and by using some mixing device installed in the test interval to keep the composition of the solution homogeneous (Kearl et al., 1988). In this test, and in the test described by Hall et al. (1991a), it was assumed that the natural turbulence in the well bore and gravel pack would provide sufficient mixing. The straight-line slopes seen in Figure 5 support this assumption. Further, the assumption was tested during the conduct of the experiment by moving the sensing electrode to four different positions in the well bore at given depths. At 11 min and at 66 min into the test, at a depth of 0.5 m below the water table, millivolt readings were made adjacent to the well screen on the upgradient side, the downgradient side, and the "left" and "right" sides. This procedure was repeated at the 8.7 m depth at 69 min and 240 min. In no case did the difference between the upgradient and downgradient measurements exceed 0.2 mv, which in the context of this experiment is negligible. Therefore, an assumption of adequate mixing must be taken as correct.

The flow through the well bore, V*, calculated from EQ (4) is related to seepage velocity within the aquifer as follows:

$$V^* = Vna \quad (5)$$

where V = seepage velocity
n = effective porosity
a = flow distortion factor

The flow distortion factor, a, arises because the hydraulic conductivity of the well is considerably greater than that of the aquifer, thereby causing the flow net (within the horizontal plane) to converge toward the well (Raymond, 1955). For this analysis, the factor will be considered invariant with depth. Because it is difficult to evaluate effective porosity variations at the various test intervals, calculation of meaningful seepage velocities for the intervals is similarly difficult. However, if the flow distortion factor is truly a constant, then V* is directly proportional to net flux (volume per unit time) for each test interval. Figure 6 illustrates the relative discharge for each test depth in relation to the 6.9-m depth, which showed the highest V*. The stratigraphy at well #4, determined by particle-size analysis of drill cuttings collected at 1.5-m intervals, is also included in the figure. The correspondence between observed stratigraphy and the results of the point-dilution test is quite good. The greatest ground-water flux is through the relatively clean sand, and the least flux is through the clayey, poorly sorted sediments.

As noted above, the point-dilution test is conventionally performed in an isolated interval. In this test and in that described by Hall et al. (1991a), there was no attempt to isolate depth intervals. It was assumed that in an aquifer dominated by horizontal advective flow, vertical mixing within the well bore would be negligible compared to horizontal flow vectors. The contrast in calculated relative discharge between the 9.6- and 10.5-m test depths in Figure 6 shows that this assumption is reasonable.

The tracer emplacement for this test also served as the beginning of a drift-and-pumpback test, as described by Hall et al. (1991b). In a drift-and-pumpback test, the tracer is allowed to drift away from the well under natural gradient for a period of days. Then, the well is pumped to recover the tracer. The time required to recover the center of mass of the tracer is then

used to calculate net seepage velocity and effective porosity of the aquifer using the following equations:

$$n = \pi b K^2 I^2 T^2 / Qt \quad (6)$$

where n = effective porosity
b = aquifer thickness 11.3 m
K = hydraulic conductivity (24.6 m/day to 28.0 m/day)
I = hydraulic gradient (0.0045)
t = pumping time to recover center of mass of tracer in days
T = drift time plus t in days
Q = pumping rate in m^3/day

and $$V = Qt / \pi b T^2 K I \quad (7)$$

where V = seepage velocity in m/day

The drift time for this test was 2.039 days. Pumping rate during recovery of the tracer was 327 m^3/day. Bromide concentration during pumping was monitored using a conventional bromide ion-selective electrode and a double-junction reference electrode. Figure 7 illustrates the results of bromide measurements. The concentration curve in the figure was integrated, and it was calculated that the center of mass of the bromide tracer was recovered after 50.6 min, or 0.0351 days. Applying EQ (6) and EQ (7) resulted in a calculated net effective porosity of 16% to 21% and net seepage velocity of 0.6 to 0.7 m/day at well #4.

DISCUSSION

The flow determined through this series of tests, 0.6 to 0.7 m/day, is greater than the apparent flow rate observed by monitoring the migration of "chill" in the aquifer during actual use of the ATES installation, which is approximately 0.45 m/day. Some difference was expected because the chill is effectively retarded by heat exchange between the injected cool water and the sediments and entrapped water of the aquifer. (The volume of entrapped water

in the sediments is reflected by the difference between effective porosity and total porosity.) Thus, in designing future ATES installations in similar sediments, or in designing the expansion to the UASRC well field, assuming a retardation coefficient of approximately 1.3 to 1.5 would be reasonable.

The effective porosity of 16% to 21% is greater than the 6% to 12% values measured for other sites in this aquifer (Cronin et al., 1989; Hall et al., 1991a). However, the higher porosity is reasonable because the hydraulic conductivity at the UASRC site is also greater. Finally, the results of the point-dilution test warrant additional comment. In EQ (5) it was shown that the mean flow velocity through the well bore, V*, is proportional to seepage velocity, V, effective porosity, n, and a flow distortion factor, a. In conventional practice, the flow distortion factor is determined by laboratory calibration of some given combination of screen and gravel pack by comparing measured V* against a known velocity, V, for a "well" established in a laboratory-scale "aquifer" (Kearl et al., 1988). Then, a velocity, V, for a real aquifer is obtained from field measurement of V* and by estimating porosity, n. That is, the flow distortion factor is considered to be strictly a function of well construction, and to be independent of the nature of the aquifer.

In this test, laboratory calibration was obviously not necessary. Velocity and porosity are known from the results of the companion tests, and the mean V* (0.91 m/day) is easily calculated from the experimental data. Therefore, from EQ (5), the flow distortion factor must be equal to approximately 7 to 8. If the flow distortion factor is truly independent of variation within the aquifer, then Figure 6 accurately depicts the relative flux, and also the relative hydraulic conductivity, for each test depth.

However, laboratory tests as well as computer simulations have shown that the flow distortion factor should be approximately 2.0 (Raymond, 1955). In this test, the value for that factor was approximately four times the expected value. Further, even higher values have been reported in the literature (Kearl et al., 1988). We interpret the disparity between laboratory experiments and field measurements as follows:

Laboratory experiments with porous media are of small scale, both in time and space, compared to real aquifers, and the media used in such experiments to simulate aquifers are often uniform and well sorted. Within the conduct of an experiment, the laboratory-scale well will not undergo significant development. (Certainly this is also true for computer simulations, where aquifer characteristics are fixed.) However, a real well is developed over time, every time it is pumped, and progressivly more fine-grained material is withdrawn from the aquifer near the well bore. That is, in the vicinity of the well, the aquifer is more conductive than the rest of the aquifer, and the sediments are better sorted.

Thus, in the laboratory tests and computer simulations, but not at a real well installation, the assumption of a uniform aquifer immediately adjacent to, and extending from, the well is a valid assumption. Therefore, the pattern of flow distortion at a real well is probably not accurately represented by the results of laboratory-scale or computer experiments.

For the present test, there is an important consequence. It is unlikely that the relative development of poorly sorted sediments, such as the material near the bottom of the aquifer, will be the same as that of the overlying sand stratum. That is, the hydraulic conductivity of well-sorted sand will be less affected by well development than the poorly sorted material, so the flow distortion factors of the two strata will probably be different. It seems intuitively likely that the relative rates of flow (i.e., the relative hydraulic conductivities) shown in Figure 6 for the poorly sorted sediments are too high compared to the sand layer. The figure must be taken as a semi-quantitative representation of the vertical distribution of flow.

Acknowledgment

This work was supported by the Pacific Northwest Laboratory, which is operated for the U.S. Department of Energy by Battelle Memorial Institute under Contract DE-AC06-76RLO 1830.

REFERENCES

Bourdet, D., J. A. Ayoub, and Y. M. Pirard (1989) "Use of pressure derivative in well-test interpretation." Paper SPE 12777, SPE Formation Evaluation, June:293-302.

Bourdet, D., T. M. Whittle, A. A. Douglas, and Y. M. Pirard (1983) "A new set of type curves simplifies well test analysis." World Oil, May:95-106.

Cronin, W. E., S. P. Luttrell, and S. H. Hall (1989). Aquifer Characterization of the Veterans Administration Hospital, Tuscaloosa, Alabama. PNL-7139, Pacific Northwest Laboratory, Richland, Washington.

Driscoll, F. G. (1986). Ground Water and Wells, 2nd Edition, Johnson Division, UOP Inc., St. Paul, Minnesota.

Hall, S. H., and D. R. Newcomer (1992). Hydrologic Characterization of the Unconfined Aquifer at the University of Alabama Student Recreation Center, Tuscaloosa, Alabama. PNL-8004, Pacific Northwest Laboratory, Richland, Washington.

Hall, S. H., D. R. Newcomer, and S. P. Luttrell (1991a). Hydrologic Characterization of the Unconfined Aquifer at the General Motors Harrison Division Plant, Tuscaloosa, Alabama. PNL-7641, Pacific Northwest Laboratory, Richland, Washington

Hall, S. H., S. P. Luttrell, and W. E. Cronin (1991b). A Method for Estimating Effective Porosity and Ground-Water Velocity, Journal of Ground Water, 29(2):171-174.

Jacob, C. E. (1946). "Drawdown Test to Determine Effective Radius of Artesian Wells." Trans. Am. Soc. Civ. Eng., 112:1047-1070.

Kearl, P. M., J. J. Dexter, and J. E. Price (1988). Procedures, Analysis, and Comparison of Groundwater Velocity Measurement Methods for Unconfined Aquifers. UNC/GJ-TMC-3, UNC Geotech, Grand Junction, Colorado.

Novakowski, K. S. (1990) "Analysis of aquifer tests conducted in fractured rock: a review of the physical background and the design of a computer program for generating type curves." Ground Water, 28(1):99-105.

Raymond, J. R. (1955). An Electrical Technique for Ground Water Velocity Measurement. HW-36217, General Electric Company, Richland, Washington.

Schaetzle, W. J., and C. E. Brett (1989). The Aquifer Chill Storage Project at the University of Alabama, Tuscaloosa: Progress Report for 1985 and 1986. PNL-6797, Pacific Northwest Laboratory, Richland, Washington.

Theis, C. V. (1935) "The relation between the lowering of the piezometric surface and the rate and duration of discharge of a well using ground-water storage." Trans. Am. Geophys. Un., 2:519-524.

SEASONAL ENERGY STORAGE

HEAT INJECTION (INITIAL)

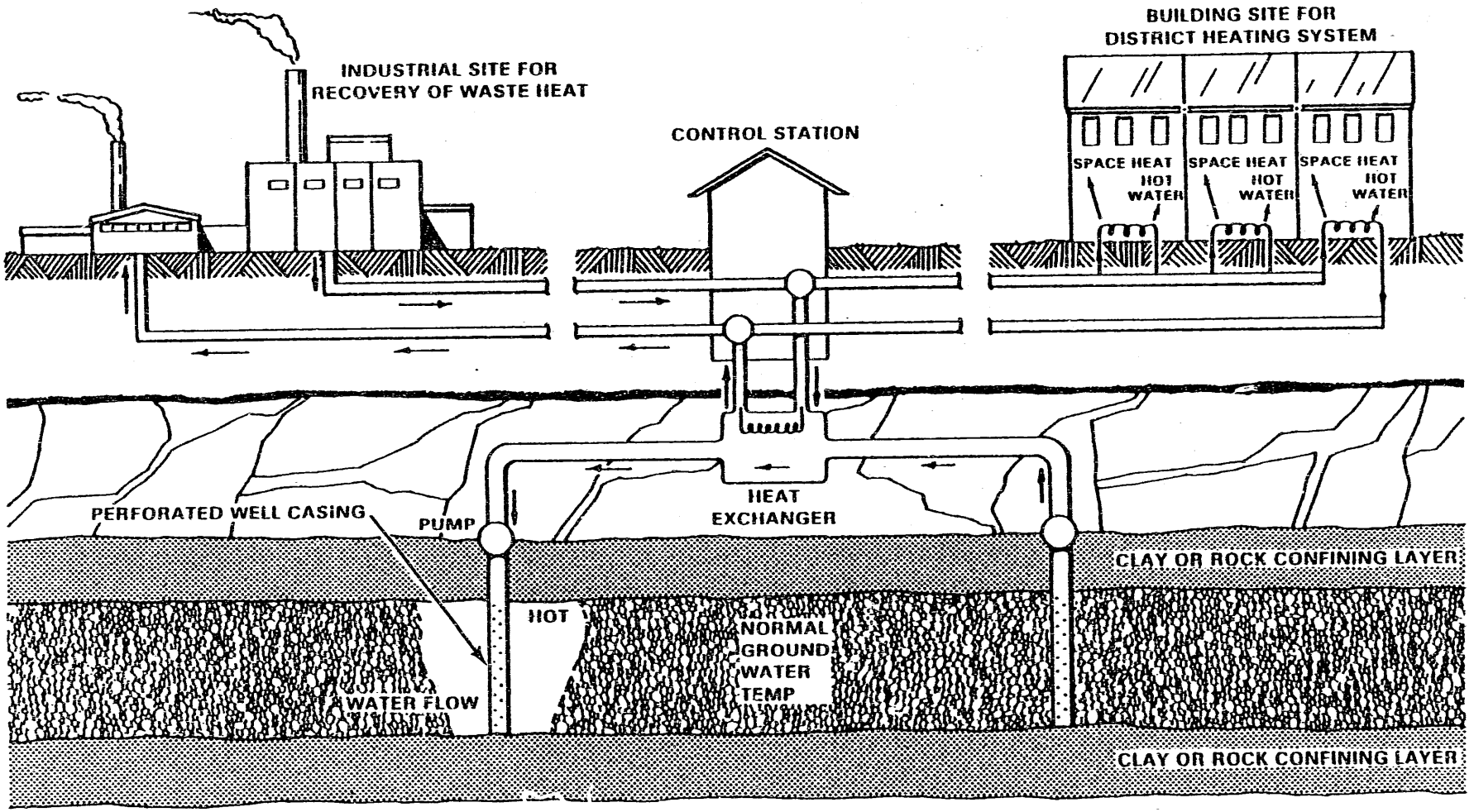

DOUBLET WELL AQUIFER STORAGE SYSTEM

FIGURE 1

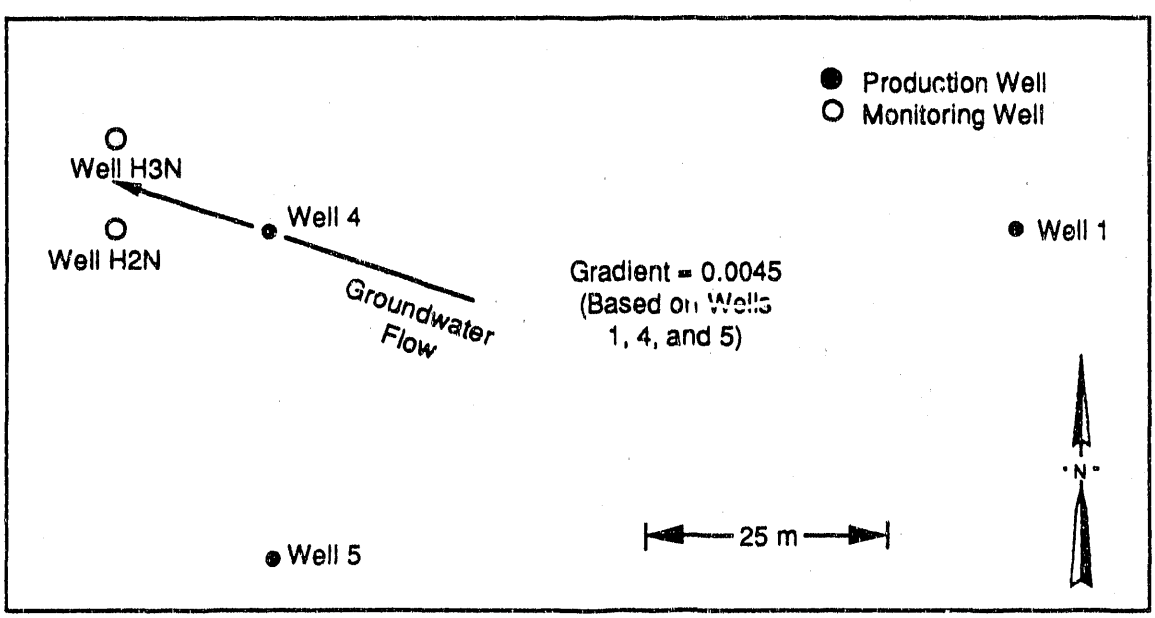

Figure 2. Well field at the University of Alabama Student Recreation Center.

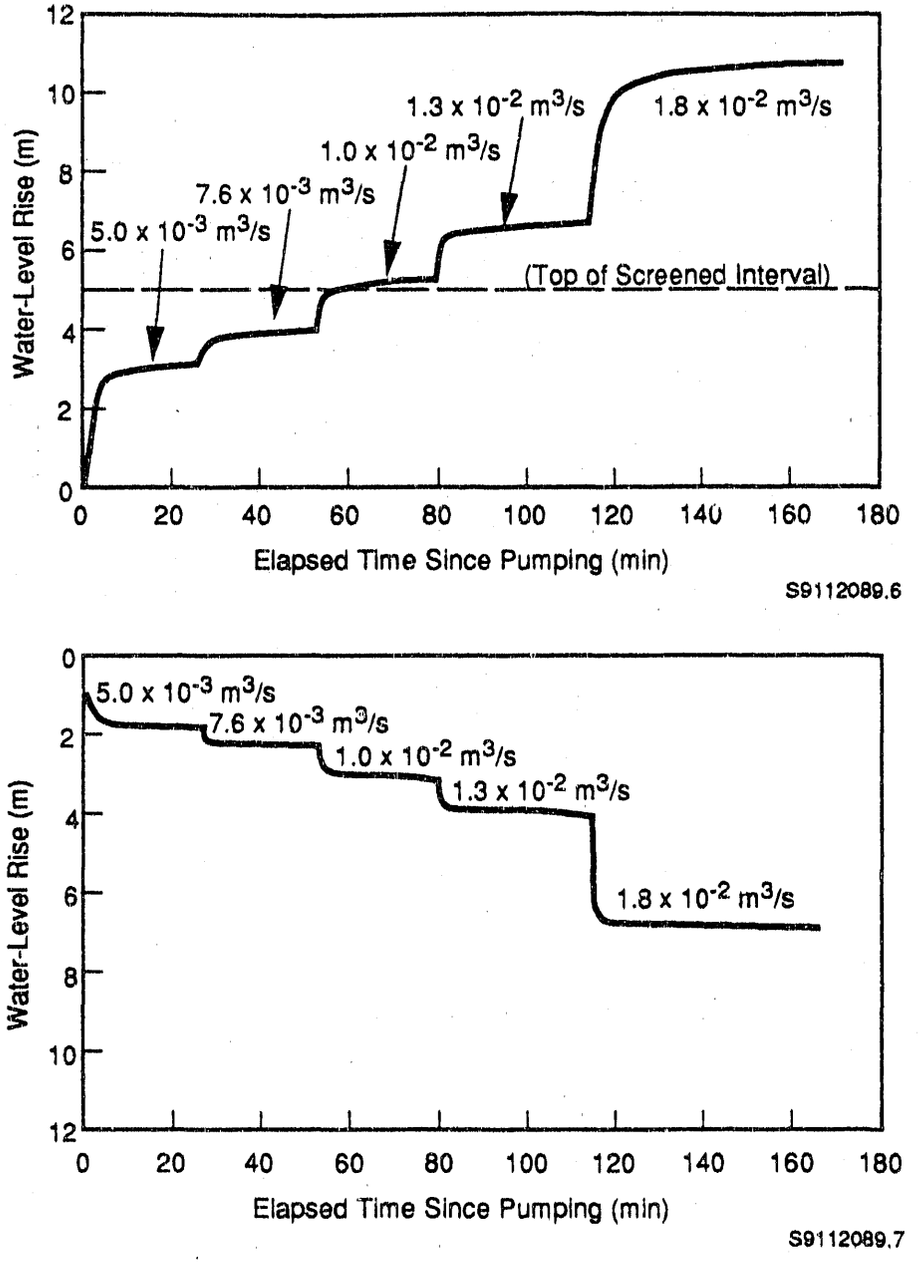

Figure 3. Water-level changes during the step-injection and step-drawdown tests.

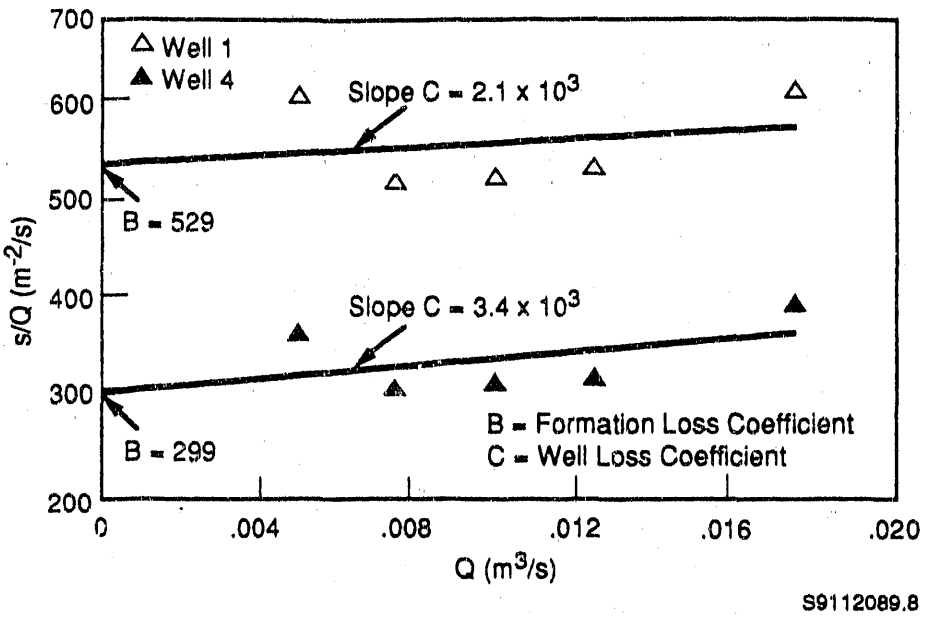

Figure 4. Change in water level normalized to pumping rate vs pumping rate for the step-injection and step-drawdown tests.

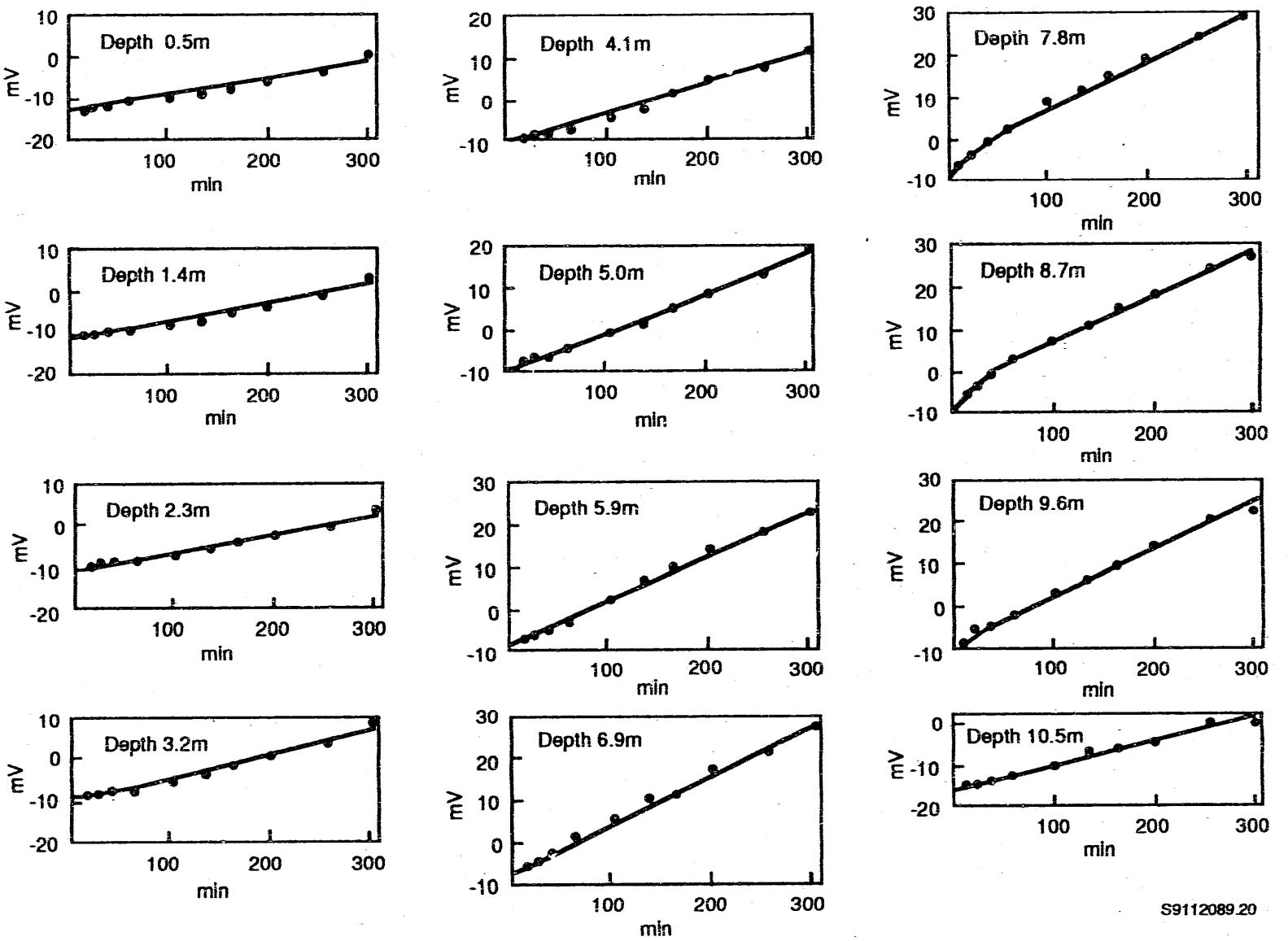

Figure 5. Bromide ion-selective electrode response at 12 depth intervals during the point-dilution test.

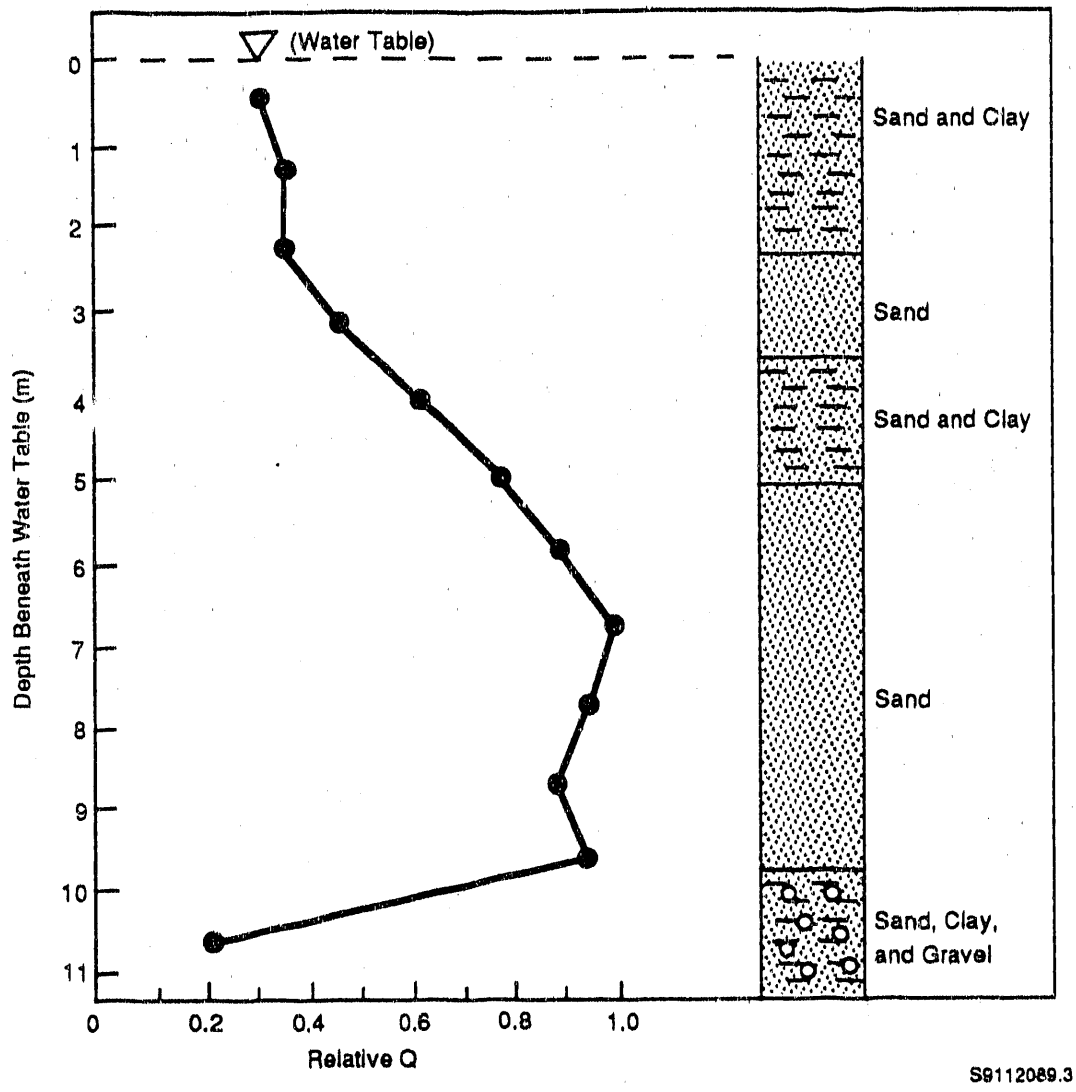

Figure 6. Relative horizontal ground water flux (Q) through the well bore at 12 depth intervals. Aquifer stratigraphy is based on examination of drill cuttings.

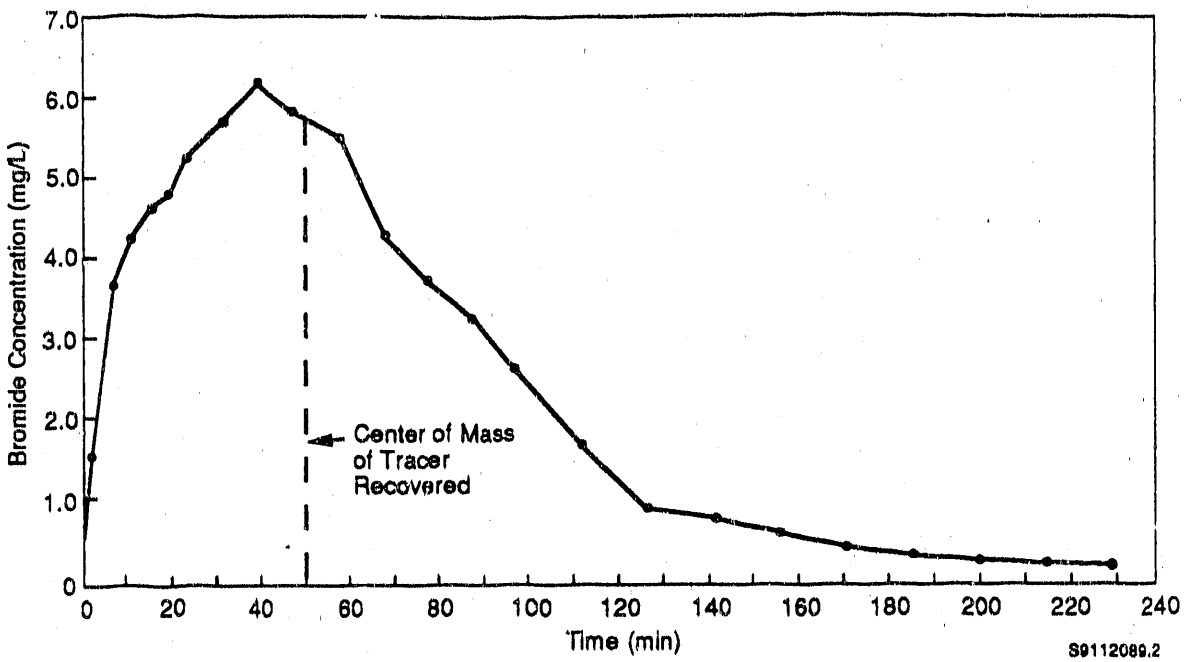

Figure 7. Bromide concentration vs time during the pumpback stage of the drift-and-pumpback test.

END

DATE FILMED

12/8/92